Supplementary Material of

Insights into Fenton-like oxidation of oxytetracycline mediated by Fe doped porous g-C$_3$N$_4$ nanomaterials: Synthesis, performance and mechanism

Xiuqin Huo [a,b], Huan Yi [a,b], Eydhah Almatrafi [b], Dengsheng Ma [a], Yukui Fu [a], Lei Qin [a], Wu Xia [a], Ling Xiang [a], Fuhang Xu [a], Huchuan Yan [a,], Chengyun Zhou [a,b], Guangming Zeng [a,b,*], Cui Lai [a,*]

[a] College of Environmental Science and Engineering and Key Laboratory of Environmental Biology and Pollution Control (Ministry of Education), Hunan University, Changsha, 410082, PR China.

[b] Center of Research Excellence in Renewable Energy and Power Systems, Center of Excellence in Desalination Technology, Department of Mechanical Engineering, Faculty of Engineering-Rabigh, King Abdulaziz University, Jeddah 21589, Saudi Arabia.

---

*Corresponding author at: College of Environmental Science and Engineering, Hunan University, Changsha, Hunan 410082, China (G.M. Zeng and C. Lai).

Tel.: +86–731– 88822754; fax: +86–731–88823701.

E-mail address: zgming@hnu.edu.cn (G.M. Zeng), laicui@hnu.edu.cn (C. Lai).

Text S1 Materials

Ferric chloride hexahydrate ($FeCl_3 \cdot 6H_2O$), Dicyandiamide (DCDA), Ethylenediamine tetraacetic Acid (EDTA), Oxytetracycline (OTC), Hydrochloric acid (HCl), Sodium hydroxide (NaOH), Hydrogen peroxide (H_2O_2), Tertiary butanol (TBA), Tetramethylpiperidinyloxy (TEMPOL) and sodium oxalate ($C_2Na_2O_4$) were of analytical grade and purchased from Sinopharm Chemical Reagent Corp (Beijing, China). All solutions were prepared by using ultrapure water with a resistivity of 18.25 MΩ.

Test S2 Characterization of Fe/PCN

Powder X-ray diffraction (XRD-6100, Cu Kα radiation, λ=0.15418 nm) was used to determine the crystal phases of Fe/PCN with the scanning range from 10° to 70°. Morphology and microstructure of the prepared samples were examined by scanning electron microscope (SEM, Zeiss Sigma 500) and transmission electron microscope (TEM, FEI Tecnai G2 f20 s-twin 200kV). The element composition of catalyst was determined through an energy-dispersive spectrometry (EDS)-elemental mapping. The surface chemical elemental compositions and valence state were examined using X-ray photoelectron spectroscopy (XPS, Thermo K-Alpha+) with Al Kα source (hv = 1486.6 eV). Fourier transform infrared (FT-IR) spectrophotometer (Perkin Elmer spectrum 100) was employed to characterize the surface functional groups. And the specific surface areas and pore volume of the prepared composites were characterized by Brunauer-Emmett-Teller (BET) method.

Test S3 Degradation intermediates identification

The degradation intermediates of OTC were identified by a LC-MS system (1290/6460 Triple Quad, Agilent) equipped with a Kromasil C18 column (250 × 4.6 mm, 5 μm). The elution was performed via 0.1% (v/v) of formic acid aqueous solution (A) and acetonitrile (B) at a flow rate of 0.2 mL min^{-1}. The injection volume was 2 μL, and the column temperature was 30 ℃. Linear gradient elution as follows: the initial 90% A was reduced to 10% A over 10 min and kept 4 min. Then the mobile phase A returned to 90% in 1 min and maintained 1min. MS was conducted in the positive ion mode using an electrospray ionization (ESI) source under the following conditions: capillary voltage, 4.0 kV; gas (N$_2$) flow rate, 11 L min^{-1}; gas temperature, 300 ℃; nebulization pressure, 15 psi. MS was scanned by mass range from 100 to 500 m/z.

Test S4 Photoelectrochemical measurement

Photoelectrochemical test was performed on electrochemical workstation (CHI760E). Sodium sulfate solution (Na$_2$SO$_4$, 0.2 M) was used as the electrolyte, and the light source was supplied by a 300 W xenon lamp (CEL-HXF300, Ceaulight) fitted with a 420 nm cutoff filter (155 mW cm^{-2}). The platinum wire was used as the counter electrode and Ag/AgCl electrode were utilized as the reference electrode. The working electrode was prepared by our photocatalyst: 0.01g of the sample was appended to 0.001 L of 25% (W/V) PVA solution and sonicated for half an hour to get suspension. Then, the suspension was coated onto a fluorine-doped tinoxide (FTO) glass (1 × 2 cm^2) which was respectively precleaned by acetone, ethanol and deionized water. Finally, the obtained electrode was laid in an oven at 110 °C for 60 min. The photocurrent-time measurement (IT) was measured on an applied voltage of 0 V with

the light on or off every 20 seconds. The electrochemical impedance spectroscopy (EIS) was collected on an applied voltage of 0 V with an amplitude of 0.005 V over a frequency between 10^{-2} and 10^5 Hz. Moreover, Mott-Schottky curve were also recorded at the frequency of 1000 Hz.
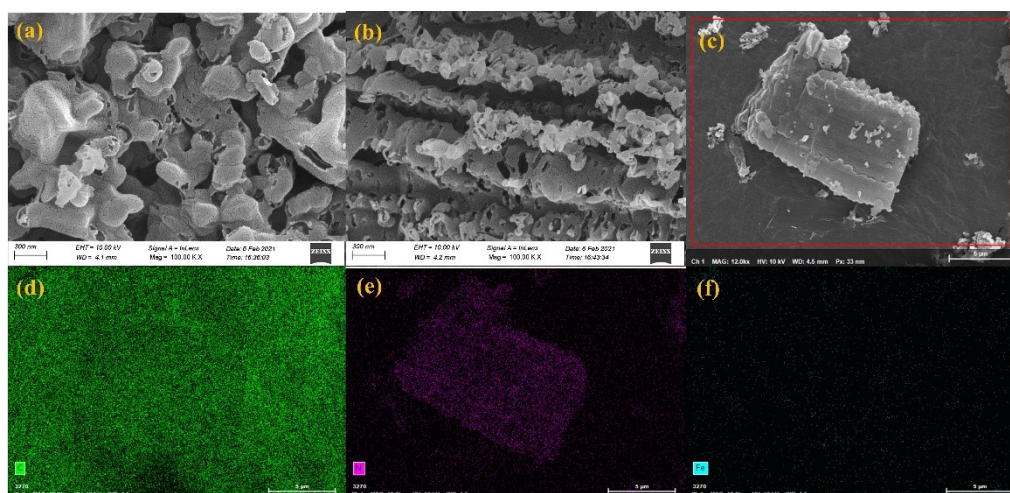

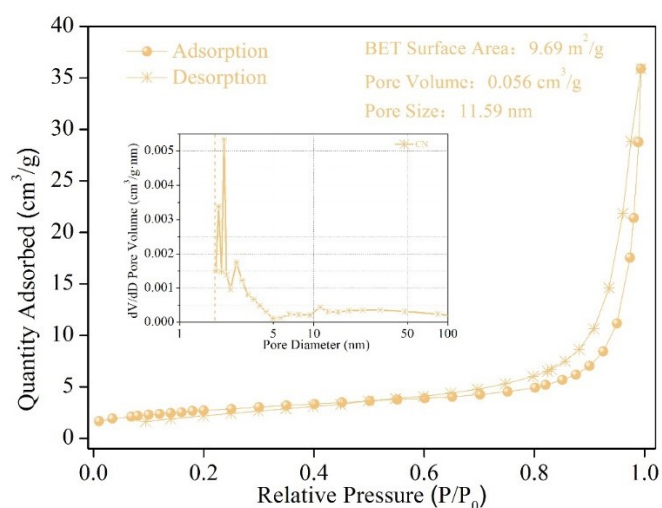Fig. S1 SEM images of (a) 0.027Fe/PCN, (b) 0.081Fe/PCN; (c-f) SEM-Mapping of 0.054Fe/PCN.

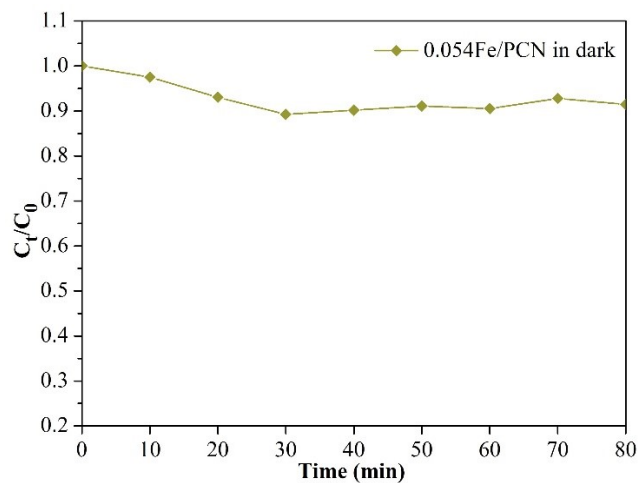Fig. S2 N$_2$ adsorption-desorption isotherms of CN, the insert image was pore size distribution curves.

Fig. S3 The adsorption equilibrium curves over 0.054Fe/PCN
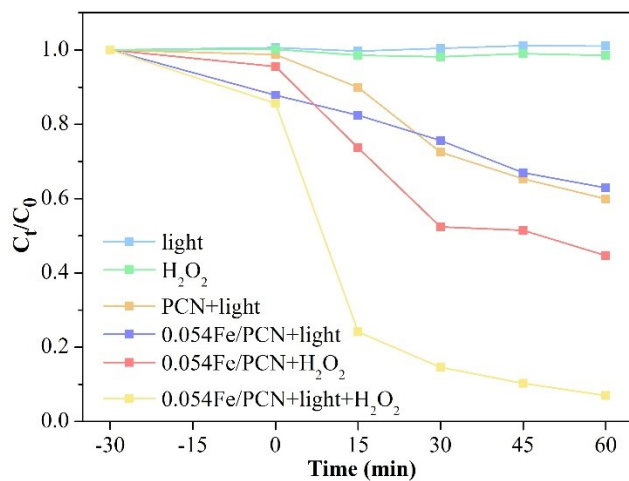
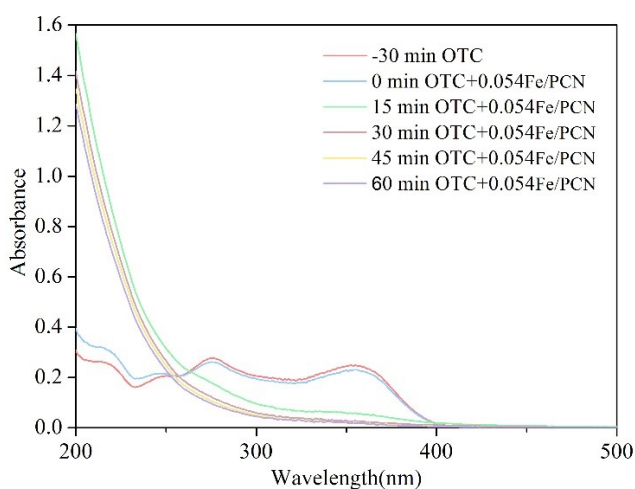Fig.S4 The OTC degradation in different condition.

Fig. S5 Time-dependent UV-Vis absorption spectra of OTC in the presence of
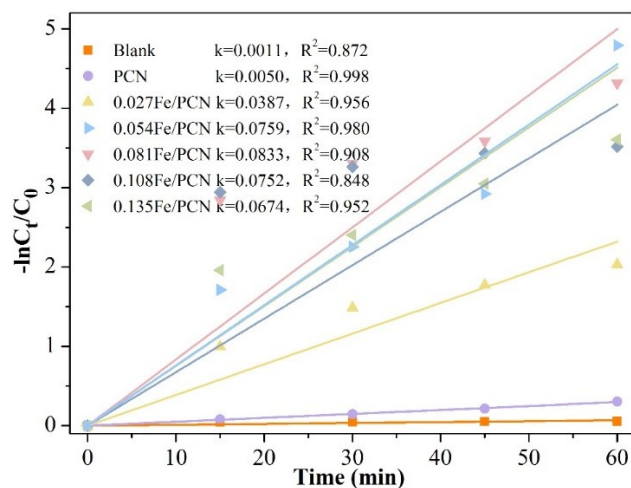
0.054Fe/PCN.

Fig. S6 The kinetics (k / min^{-1}) of OTC under visible light by PCN and xFe/PCN.
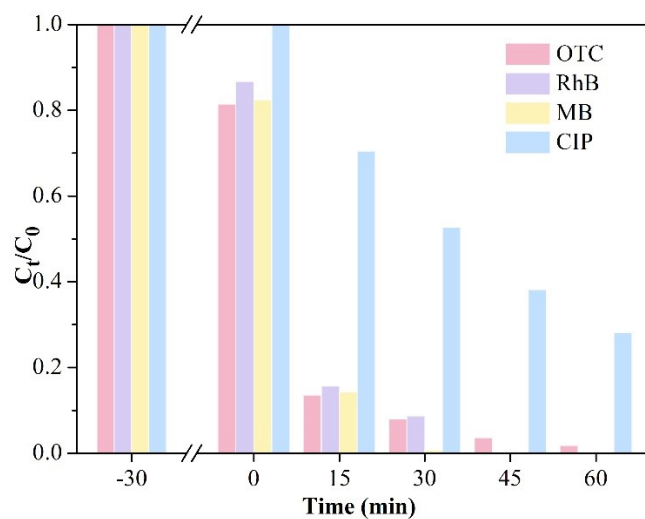

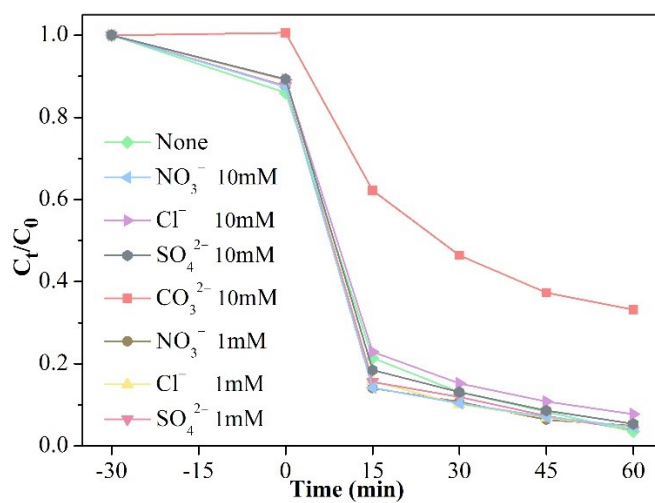Fig. S7 The degradation for different organics over 0.054Fe/PCN.

Fig. S8 The OTC degradation with different concentration of inorganic salt ions.
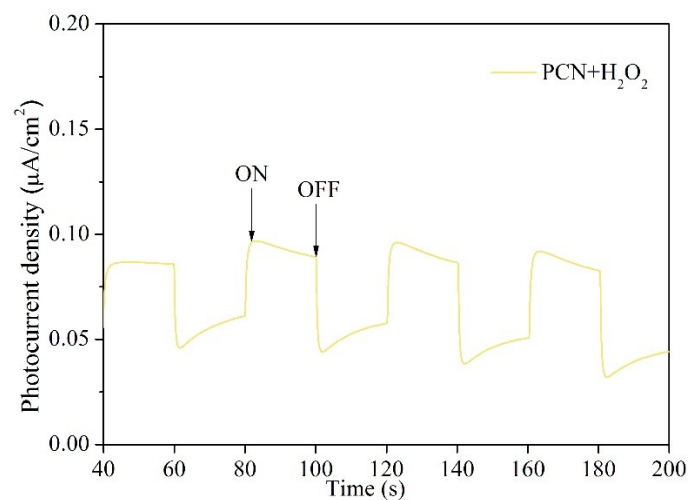
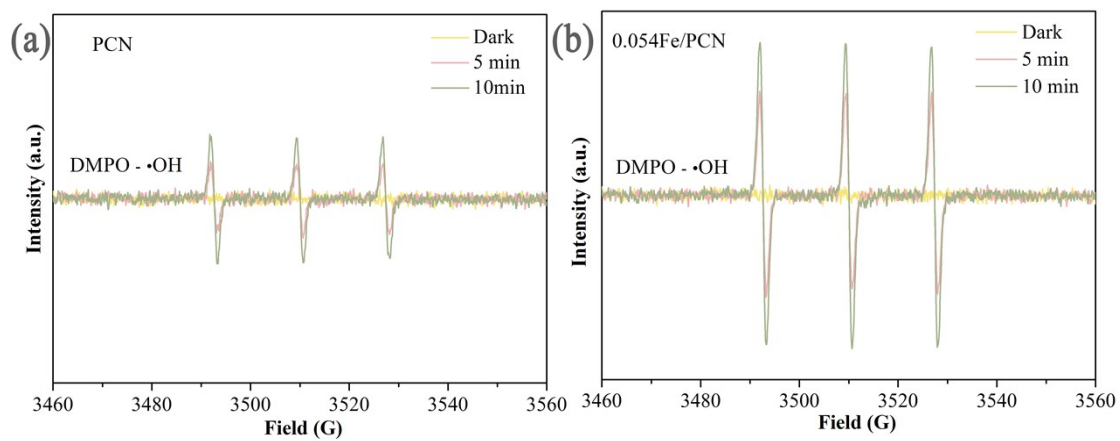Fig. S9 The transient photocurrent-time response curves of PCN and PCN+H_2O_2.

Fig. S10 DMPO-•OH signal of PCN+H_2O_2 and 0.054Fe/PCN+H_2O_2 in dark and

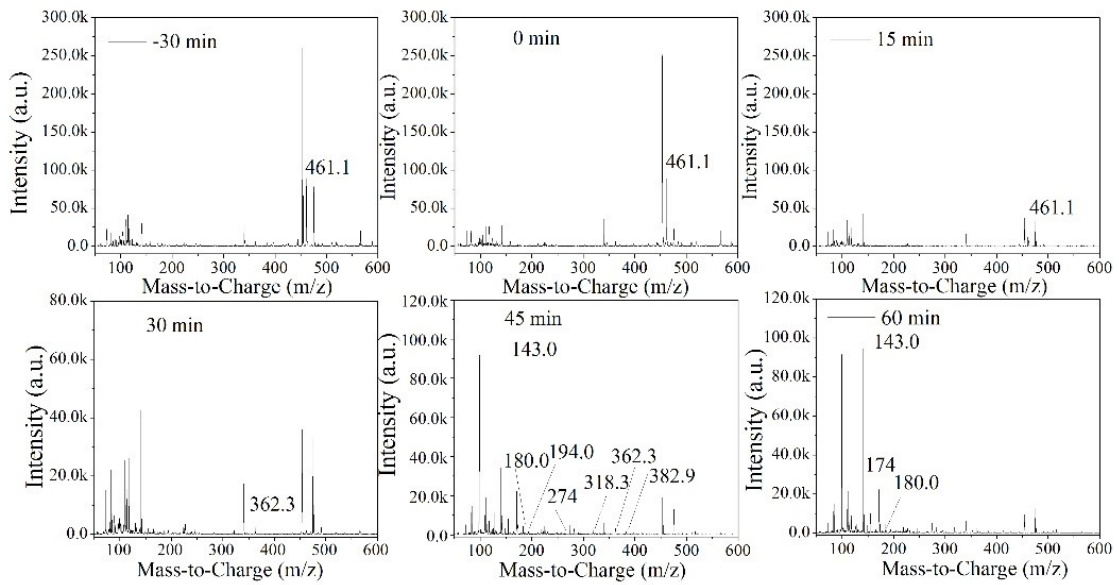visible-light irradiation. (0 min represents dark condition)

Fig. S11 LC-MS spectra of the OTC intermediates eluted in the degradation process: (a) original OTC solution, (b) after 30 min adsorption, (c) light on 15 min, (d) light on 30 min, (e) light on 45 min, (f) light on 60 min.
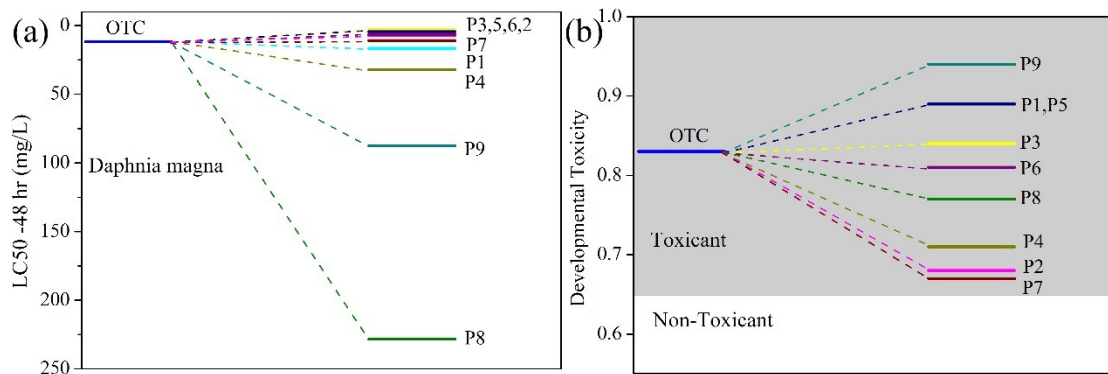

Fig. S12 (a) Daphnia magna LC50-48hr; (b) the developmental toxicity of OTC and predictive intermediates.
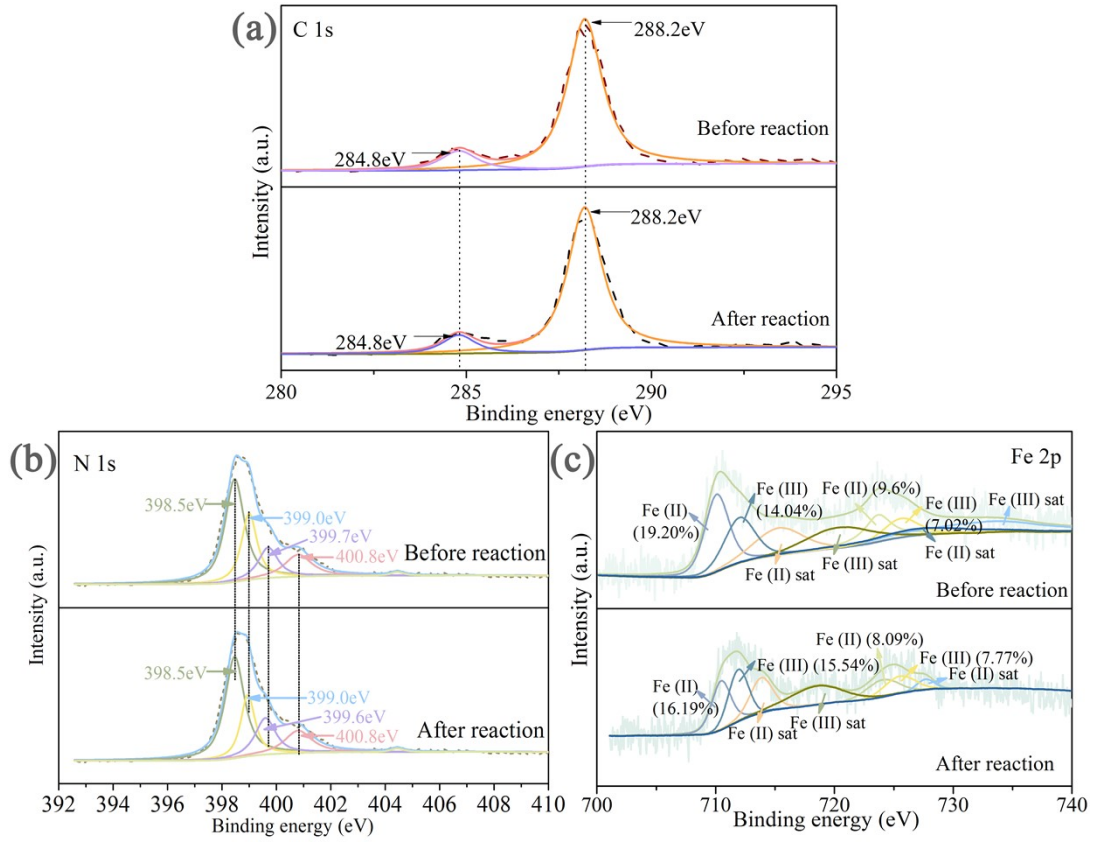
Fig. S13 XPS spectrum of (a) C, (b) N and (c) Fe of fresh and used 0.054 Fe/PCN.
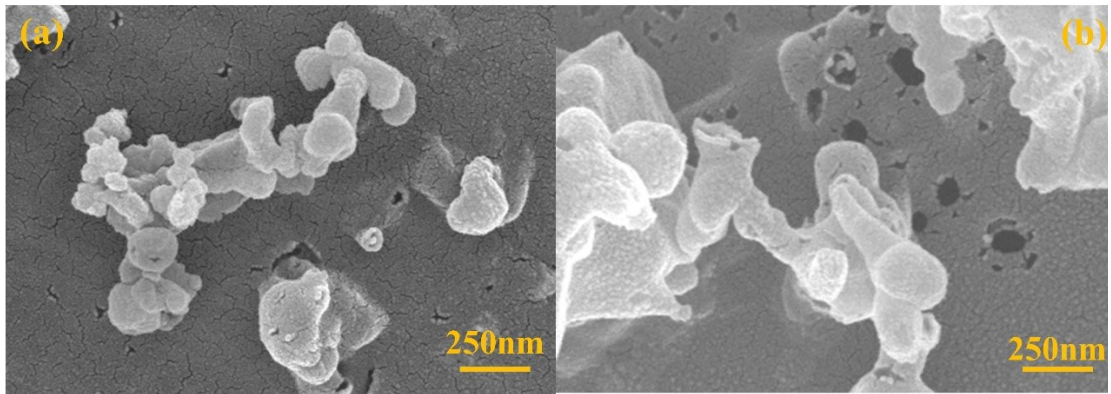

Fig. S14 The morphology of (a) fresh and (b) used 0.054 Fe/PCN.

Table S1 The element content (at%) of PCN, 0.054Fe/PCN determined by XPS.

Samples	C	N	O	C/N
PCN	43.34	53.3	3.36	81.31
0.054Fe/PCN	40.59	49.81	8.21	81.49

Table S2 Proportion of different chemical bonds about C atoms in different samples.

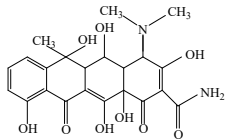| Samples	defective C–C	N=C–N
PCN	5.21%	94.79%
0.054Fe/PCN	11.49%	88.51%
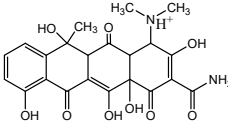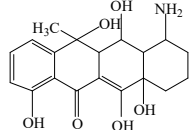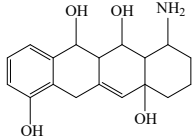
Table S3 Proportion of different chemical bonds about N atoms in different samples.

Samples	C=N–C	N–(C)$_3$	N–H$_x$	Fe-N	π–π* excitations
PCN	44.21%	39.67%	15.84%		0.28%
0.054Fe/PCN	46.72%	24.00%	14.06%	14.04%	1.18%

Table S4 Comparison of the catalytic performance of 0.054 Fe/PCN and other catalysts.

Catalysts	Dosage	Organics	C_{Org} (ppm)	C_{H2O2} (mM)	Time (min)	conversion	Ref
$MnFe_2O_4/g-C_3N_4$	0.25g/L	OTC	30	125	60	80.5%	[1]
$ErFeO_3/g-C_3N_4$	0.5g/L	OTC	20	50	80	99.7%	[2]
$Bi_2WO_6/CoAl-LDHs$	1 g/L	OTC	10	50	60	98.47%	[3]
CuFeO QDs/CNNSs	0.5g/L	TC	50	100	25	99.8%	[4]
FeTi/CN	0.1 g/L	OTC	10	20	60	98%	[5]
$FePc/g-C_3N_4$	0.125 g/L	OTC	10	12.5	60	88.48 %	[6]
$Cu_{0.5}Mn_{0.5}Fe_2O_4$	0.5g/L	OTC	46	97.89	120	100%	[7]
$FeMo_3O_x/g-C_3N_4$	1.33 g/L	TC	25	20	60	100%	[8]
	1.33 g/L	OTC	25	20	60	97.1%	
$MgFe_2O_4@g-C_3N_4$	0.5 g/L	TC	20	80	60	90.79%	[9]
Fe/PCN	0.2 g/L	OTC	10	5	60	99.2%	This work

Table S5 Information of the intermediates.

Compounds	Formula	m/z	Proposed structure
OTC	$C_{22}H_{24}N_2O_9$	461	
P1	$C_{21}H_{21}NO_6$	383	
P2	$C_{19}H_{23}NO_6$	362	
P3	$C_{18}H_{23}NO_4$	318	

P4	$C_{15}H_{18}O_5$	279	
P5	$C_{18}H_{24}O_2$	274	
P6	$C_{12}H_{16}O_2$	192	
P7	$C_{11}H_{14}O_2$	178	
P8	$C_{10}H_{20}O_2$	172	
P9	$C_9H_{18}O$	142	

Reference

1. H. Sun, T. Zhou, J. Kang, Y. Zhao, Y. Zhang, T. Wang and X. Yin, High-efficient degradation of oxytetracycline by visible photo-Fenton process using MnFe2O4/g-C3N4: Performance and mechanisms, *Separation and Purification Technology*, 2022, **299**, 121771.

2. L. Wang, X. Ran, B. Xiao, L. Lei, J. Zhu, X. Xi, G. Feng, R. Li and J. Feng, Visible light assisted Fenton degradation of oxytetracycline over perovskite ErFeO3/porous g-C3N4 nanosheets p-n heterojunction, *Journal of Environmental Chemical Engineering*, 2022, **10**, 108330.

3. B. Shao, Z. Liu, L. Tang, Q. Liang, Q. He, T. Wu, Y. Pan, M. Cheng, Y. Liu, X. Tan, J. Tang, H. Wang, H. Feng and S. Tong, Construction of Bi2WO6/CoAl-LDHs S-scheme heterojunction with efficient photo-Fenton-like catalytic performance: Experimental and theoretical studies, *Chemosphere*, 2022, **291**, 133001.

4. M. Liu, H. Xia, W. Yang, X. Liu, J. Xiang, X. Wang, L. Hu and F. Lu, Novel Cu-Fe bi-metal oxide quantum dots coupled g-C_3N_4 nanosheets with H_2O_2 adsorption-activation trade-off for efficient photo-Fenton catalysis, *Applied Catalysis B: Environmental*, 2022, **301**, 120765.

5. C. Lai, D. Ma, H. Yi, M. Zhang, F. Xu, X. Huo, H. Ye, L. Li, L. Yang, L. Tang and M. Yan, Functional partition of Fe and Ti co-doped g-C3N4 for photo-Fenton degradation of oxytetracycline: Performance, mechanism, and DFT study, *Separation and Purification Technology*, 2023, **306**, 122546.

6. F. Xu, C. Lai, M. Zhang, D. Ma, L. Li, S. Liu, X. Zhou, H. Yan, N. Wang, M. Xu, L. Qin and H. Yi, Graphite carbon nitride coupled with high-dispersed iron (II) phthalocyanine for efficient oxytetracycline degradation under photo-Fenton process: Performance and mechanism, *Separation and Purification Technology*, 2023, **308**, 122829.

7. A. Angkaew, C. Sakulthaew, M. Nimtim, S. Imman, T. Satapanajaru, N. Suriyachai, T. Kreetachat, S. Comfort and C. Chokejaroenrat, Enhanced Photo-

Fenton Activity Using Magnetic Cu0.5Mn0.5Fe2O4 Nanoparticles as a Recoverable Catalyst for Degrading Organic Contaminants, *Water*, 2022, **14**, 3717.

8.　　Y. Liu, X. Wang, Q. Sun, M. Yuan, Z. Sun, S. Xia and J. Zhao, Enhanced visible light photo-Fenton-like degradation of tetracyclines by expanded perlite supported FeMo3Ox/g-C3N4 floating Z-scheme catalyst, *Journal of Hazardous Materials*, 2022, **424**, 127387.

9.　　S. Qiu, L. Gou, F. Cheng, M. Zhang and M. Guo, Novel heterostructured metal doped MgFe2O4@g-C3N4 nanocomposites with superior photo-Fenton preformance for antibiotics removal: One-step synthesis and synergistic mechanism, *Journal of Environmental Management*, 2022, **321**, 115907.